

# Solar Radio-Frequency Reflectivity and Localization of FRB from Solar Reflection

S. Wang<sup>1</sup> & J. I. Katz,<sup>2\*</sup>

<sup>1</sup>*Department of Physics, Washington University, St. Louis, Mo. 63130 USA*

<sup>2</sup>*Department of Physics and McDonnell Center for the Space Sciences, Washington University, St. Louis, Mo. 63130 USA*

18 October 2022

## ABSTRACT

The radiation of a Fast Radio Burst (FRB) reflects from the Moon and Sun. If a reflection is detected, the time interval between the direct and reflected signals constrains the source to a narrow arc on the sky. If both Lunar and Solar reflections are detected these two arcs intersect, narrowly confining the location on the sky. A previous paper calculated reflection by the Moon. Here we calculate the reflectivity of the Sun in the “flat Sun” approximation as a function of angle of incidence and frequency. The reflectivity is high at low frequencies ( $\lesssim 100$  MHz) and grazing incidence (angles  $\gtrsim 60^\circ$ ), but exceeds 0.1 for frequencies  $\gtrsim 80$  MHz at all angles. However, the intense thermal emission of the Solar corona likely precludes detection of the Solar reflection of even MJy Galactic bursts like FRB 200428.

**Key words:** radio continuum, transients: fast radio bursts, Sun: atmosphere

## 1 INTRODUCTION

The all-sky FRB rate, above a threshold  $\sim 1$  Jy-ms at 1400 MHz, is  $\sim 10^6$ /sky-year (Cordes & Chatterjee 2019; Petroff, Hessels & Lorimer 2022). Despite this, until recently only  $\sim 100$  distinct FRB sources had been observed (Petroff *et al.* 2016; Transient Name Server) because most radio telescopes have very limited fields of view. For example, an individual Parkes beam has a width of about  $10^{-5}$  sterad at this frequency; its 13 beams together cover about  $10^{-5}$  of the sky. CHIME/FRB (Ng *et al.* 2017; CHIME/FRB Collaboration 2021a) has the comparatively large field of view of 200 square degrees and discovered 536 distinct FRB sources above a 400–800 MHz fluence threshold of about 5 Jy-ms in about a year (CHIME/FRB Collaboration 2019b; Fonseca *et al.* 2020; CHIME/FRB Collaboration 2021b). STARE2, consisting of a network (providing interferometric localization information) of choke-ring (essentially dipole) feeds (Bochenek *et al.* 2020a), has a field of view of about 3.6 sterad, about 30% of the sky, at the price of the very high L-band detection threshold of  $\sim 300$  kJy-ms.

It has long been realized (Katz 2014) that a “cosmological” FRB in our Galaxy would be bright enough to be observed by a single half-wave dipole antenna, and that a small network of such dipoles could localize it. STARE2 observed (Bochenek *et al.* 2020b) the first (at the time of writing, only) Galactic FRB 200428, even though it was less energetic than any observed extra-Galactic FRB. It was also, more fortuitously, observed by CHIME/FRB (CHIME/FRB Collaboration 2020a). More FRB with accurate positions, as well as observations with full-sky sensitivity, could identify future Galactic FRB.

A radio telescope whose beam is approximately matched to the angular size of the Moon or the somewhat larger (Mercier & Chambe 2015) radio size of the Sun (telescope diameter about 22 m in L-band) and staring at that object could detect reflected radiation from a FRB anywhere in the sky, with sensitivity about one order of magnitude less than that of a dipole or a single element of STARE2. Although insufficiently sensitive to detect FRB at cosmological distances, this was proposed (Katz 2020) as a method to detect Galactic micro-FRB, and anticipated the the first such event discovered, FRB 200428.

Greater sensitivity could be provided by a larger telescope with a multi-beam feed covering the Moon or Sun. Comparing the phases of the signals from such telescopes with that from STARE2 or a similar instrument would provide two very long interferometric baselines, one equal to the projected Earth-Moon separation and one equal to the projected Earth-Sun separation, and would therefore enable precise localization on the sky. At the lower frequencies at which the Solar reflectivity is high, the resolution-matched telescope would be much larger than 22 m and its sensitivity higher, but even a 22 m telescope could have useful sensitivity.

This paper calculates the reflectivity of the Sun as a function of frequency and angle of incidence using a known model of the Solar atmosphere and corona. The reflectivity must be known to evaluate the feasibility of observing FRB reflected by the Sun. The geometry is shown in Fig. 1. Qualitative refracted ray paths were shown by Newkirk (1961) before the development of modern quantitative coronal models.

## 2 REFLECTIVITY

Katz (2020) estimated that the radio-frequency reflectivity

\* E-mail katz@wuphys.wustl.edu

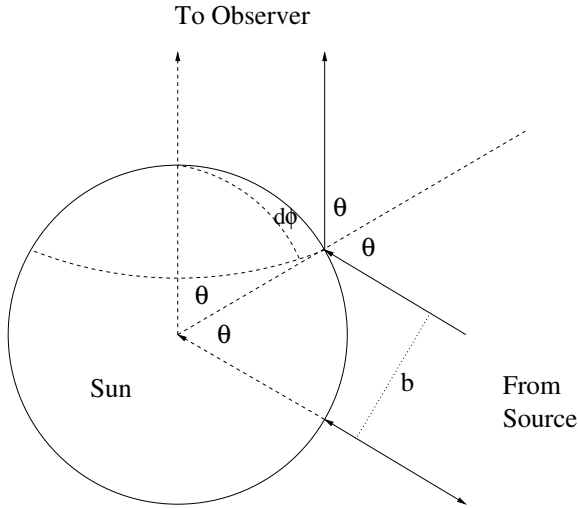


**Figure 1.** Scattering of FRB radiation by the Sun (after Fig. 1 of Katz (2020); asymptotes of the ray paths are shown). The angle of incidence is  $\theta$ .

of the Sun is low at frequencies  $\gtrsim 200$  MHz, but high at lower frequencies. FRB have not generally been observed at low frequencies, in part because dispersion delays and scattering broadening are much greater at low frequencies, the former scaling  $t_{\text{dispersion}} \propto \nu^{-2}$  (and the derivative that measures the differential arrival time across a channel  $dt_{\text{dispersion}}/d\nu \propto \nu^{-3}$ ), and  $dt_{\text{scatter}}/d\nu \propto \nu^{-4}$ . However, FRB 20180916B was detected by LOFAR at frequencies as low as 120 MHz (Pastor-Marazuela *et al.* 2020; Pleunis *et al.* 2021), demonstrating that at least some FRB may be observed at these low frequencies at which the Solar reflectivity is expected to be high.

Radar measurements of the Solar reflectivity only measure it at normal incidence, but most FRB specularly reflected by the Sun to the Earth will have angles of incidence far from normal, so their rays do not penetrate the denser and more absorptive lower layers of the Solar atmosphere.

Radio telescopes operating at lower frequencies ( $< 300$  MHz), such as the Murchison Widefield Array (Tingay *et al.* 2013; Wayth *et al.* 2018), LOFAR (van Haarlem *et al.* 2013) and the planned SKA LFAA (de Lera Acedo *et al.* 2020), are generally phased arrays of dipoles. Focusing is electronic (beams are synthesized) so the telescope can effectively “stare” at the Sun without imposing a focussed visible and infrared light heat load on the receiving elements. The older Giant Metrewave Radio Telescope (Ananthakrishnan 1995) uses parabolic dishes to focus radio waves, but its dishes are made of an open (7% filled) wire mesh that does not efficiently focus visible light because the wires are cylindrical and much thicker than the wavelength of visible light. If necessary, the receiver can be protected from focussed sunlight with a thin sheet of opaque (to visible and infrared light) plastic.

Synthesized beams have complex angular structure, rather than being simply matched to the angular size of the Sun, as would be possible for a parabolic dish at shorter wavelengths and proposed for parabolic reflectors staring at the Moon at higher frequencies. Despite this, they are sensitive to FRB scattered by the Sun; aside from radio frequency interference (generally narrowly confined in frequency), there is little radiation with the temporal characteristics of FRB in

any direction, other than FRB themselves. At low frequencies the dispersion and scatter broadening characteristic of FRB are large, making them easy to discriminate from any other transients in a synthesized beam. Solar-scattered FRB would be distinguishable from unscattered FRB simultaneously observed in other lobes of the beam by different dispersion measures and by the possible earlier direct path observation of flux from the FRB by instruments like STARE2.

The reflectivity

$$\mathcal{R}(\nu, \theta) = \exp(-\tau(\nu, \theta)), \quad (1)$$

where  $\nu$  is the wave frequency and  $\theta$  is determined by the direction to the FRB. The absorption optical depth along the ray path

$$\tau(\nu, \theta) = \int \kappa(\nu, n_e(\vec{r}), T(\vec{r})) ds, \quad (2)$$

where  $\kappa(\nu, n_e, T)$  is the opacity, the electron density  $n_e = n_e(\vec{r})$  and the temperature  $T(\vec{r})$  are found from a model (Newkirk 1967) of the Solar corona.

The path  $\vec{r}(s)$  of a ray of radiation is found, in the geometrical optics limit, from the eikonal equation (Braun 2004)

$$\frac{d}{ds} \left( n \frac{d\vec{r}}{ds} \right) = \vec{\nabla} n, \quad (3)$$

where  $ds$  is an element of path length, the refractive index

$$n = \sqrt{1 - \frac{\omega_p^2}{\omega^2}}, \quad (4)$$

$\omega = 2\pi\nu$  and the plasma frequency

$$\omega_p = \sqrt{\frac{4\pi n_e e^2}{m_e}}. \quad (5)$$

For a specified  $n_e(\vec{r})$ , we integrate Eq. 3 numerically to find the path. In a “flat Sun” approximation the initial condition is the angle of incidence  $\theta$  at an altitude far above the Solar surface, where  $\omega_p \ll \omega$  and refraction is negligible. This is related to the impact parameter  $b$  by  $b = b(\theta)$ . In general this relation is non-trivial, but in a “flat Sun” approximation  $b = R \sin \theta$ , where  $R$  is the Solar radius and  $\vec{r}$  is replaced by an altitude  $z$ . This approximation is justified because a 150 MHz ray at near-normal incidence penetrates, fitting the profile of Newkirk (1967), to an altitude  $\approx 0.04R_\odot$  above the photosphere, where the scale height of the Solar atmosphere  $\approx 0.09R_\odot$ . At shallower angles of incidence the penetration is shallower, the attenuation less, and its quantitative calculation less important.

There is an extensive literature on the properties of the Solar corona (*e.g.* Saito, Poland & Munro (1977); Geryaev *et al.* (2014); McCauley, Cairns & Morgan (2018); Zhang, Wang & Kontar (2021)). Unfortunately, only a fraction of this literature is concerned with the background Solar corona (as opposed to phenomena such as coronal streamers or Type III radio bursts) and apparently none provides both the density and the temperature in the inner coronal region relevant here. Instead, we fit the smooth density profile of an isothermal quiet Solar corona

$$n_e(r) = n_0 \exp\left(\frac{GM\mu}{k_B T r}\right) \quad (6)$$

to the classic results of Newkirk (1967), where the molecular

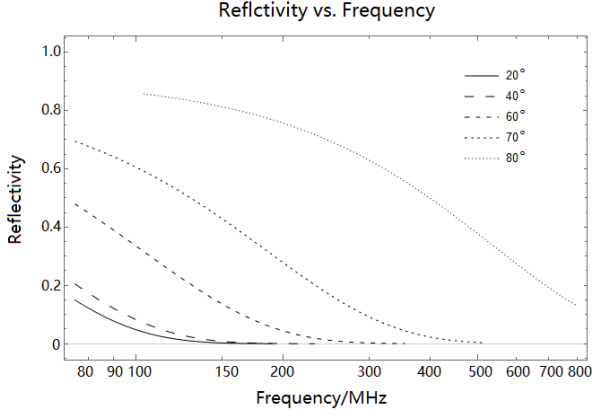


**Figure 2.** Solar reflectivity *vs.* frequency at several angles of incidence  $\theta$ .

weight  $\mu$  per particle is taken as  $0.6m_p$ , where  $m_p$  is the proton mass, appropriate to fully ionized hydrogen and helium. A good fit is obtained for  $T = 1.1 \times 10^6$  K, a value we adopt to calculate the opacity.

More detailed modern studies (Mercier & Chambe 2015) show that even the quiet corona is both very variable and not spherically symmetric. Because the present work is only a feasibility study whose purpose is to estimate whether Solar-reflected FRB may be observable, we do not need very accurate temperature and density profiles; the variability of the corona makes any model profile only approximately applicable at any particular time and for any particular direction to a FRB. If reflected FRB are observed the quantity of interest will be the time delay between the direct and reflected signals, not their comparative amplitudes.

The opacity (Spitzer 1962), including the effect of stimulated emission,

$$\begin{aligned} \kappa(\nu, n_e, T) &= \frac{4}{3} \sqrt{\frac{2\pi}{3k_B T}} \frac{n_e \sum_Z n_Z Z^2 e^6}{h c m_e^{3/2} \nu^3} \\ &\quad \left\{ 1 - \exp \left[ - \left( \frac{h\nu}{k_B T} \right) \right] \right\} g_{ff} \\ &\approx \frac{4}{3} \sqrt{\frac{2\pi}{3}} \frac{n_e \sum_Z n_Z Z^2 e^6}{(k_B T m_e)^{3/2} c \nu^2} g_{ff}, \end{aligned} \quad (7)$$

where  $n_Z$  is the density of ions with charge  $Z$  (allowing for multiply ionized atoms in the hotter regions),  $k_B$  is the Boltzmann constant and  $g_{ff}$  is the Gaunt factor. The Gaunt factor depends only logarithmically on the parameters, except where  $\omega \rightarrow \omega_p$  and the group velocity is significantly less than  $c$  (Spitzer 1962), and is typically about 15 (van Hoof *et al.* 2014). Rays whose angles of incidence are not small do not closely approach  $\omega = \omega_p$ . Eqs. 1, 2 are then used to find the reflectivity.

The results for several angles of incidence are shown as functions of the frequency in Fig. 2 and as functions of the angle of incidence in Fig. 3.

### 3 SOLAR BACKGROUND

In addition to scattered FRB, a telescope pointed at the Sun receives Solar radiation, with which the FRB signal must

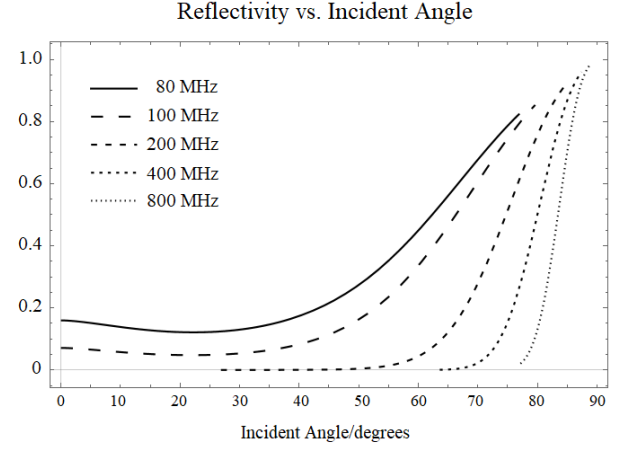


**Figure 3.** Solar reflectivity *vs.* angle of incidence at several frequencies.

compete. At the frequencies of interest, 100–200 MHz, the quiet Sun is nearly a thermal emitter at its coronal temperature with a brightness temperature  $T_b \sim 10^6$  K, corresponding to a flux  $F_{b,\nu} \sim 10^4$  Jy (Kraus 1966). During periods of Solar activity  $T_b$  may be much higher; scattered FRB cannot be detected at such times. If the Sun fills the field of view (or the resolution element of a larger telescope), the background quiet Sun antenna temperature  $T_b \sim 10^6$  K. A telescope staring at the Moon has  $T_b \approx 235$  K, its mean surface temperature.

A FRB (or other distant source) with direct flux  $F_\nu$  produces a scattered flux at the Earth (Katz 2020)

$$F_{scatt} = \frac{\mathcal{R}(\theta, \nu)}{4} \frac{R^2}{D^2} \cos \theta F_\nu \approx 5 \times 10^{-6} \mathcal{R}(\theta, \nu) \cos \theta F_\nu, \quad (8)$$

where  $\mathcal{R}(\theta, \nu)$  is the reflectivity calculated in Sec. 2,  $\theta$  is the angle of incidence,  $R = R_\odot$  the radius of the scattering object,  $D = 1$  AU its distance and  $F_\nu$  is the unscattered flux ( $R/D$  is nearly the same for the Moon and the Sun).

For a telescope matched to the angular size of the Sun with diameter  $d = \lambda D/2R$ , the antenna temperature produced by the scattered radiation

$$\begin{aligned} k_B T_{scatt} &= \frac{\pi}{4} d^2 F_{scatt} \\ &= \frac{\pi}{4} d^2 \frac{\mathcal{R} \cos \theta}{4} \left( \frac{R}{D} \right)^2 F_\nu \\ &= \frac{\pi}{16} \mathcal{R} \cos \theta \lambda^2 F_\nu \end{aligned} \quad (9)$$

or

$$T_{scatt} \approx 1300 \mathcal{R} \cos \theta \left( \frac{100 \text{ MHz}}{\nu} \right)^2 \frac{F_\nu}{1 \text{ MJy}} \text{ K}. \quad (10)$$

For a matched telescope the antenna temperature  $T_{scatt}$  is independent of the angular size of the scatterer. At  $\nu = 100$  MHz such a telescope would have  $d \approx 350$  m, which is not feasible. For a more feasible telescope with  $d = 25$  m

$$T_{scatt} \approx 7 \mathcal{R} \cos \theta \frac{F_\nu}{1 \text{ MJy}} \text{ K}. \quad (11)$$

The limiting factor in observations in the direction of the Sun is not the receiver noise temperature but the thermal emission from the corona, that may be approximated as a

black body of temperature  $T_{corona} \sim 10^6(1-\mathcal{R})$  K, where the physical temperature  $\sim 10^6$  K is multiplied by the emissivity  $1 - \mathcal{R}$ . Integrated over a bandwidth  $B$  and a time (such as the duration of a FRB)  $\Delta t$ , the signal to (background) noise ratio of detection

$$\begin{aligned} \frac{S}{N} &\approx \frac{T_{scatt}}{T_{corona}} \sqrt{B\Delta t} \\ &\sim 0.003 \frac{F_\nu}{1 \text{ MJy}} \sqrt{\frac{B\Delta t}{100 \text{ MHz-ms}}} \frac{\mathcal{R}}{1-\mathcal{R}}. \end{aligned} \quad (12)$$

In addition, scattering in the turbulent corona would temporally broaden a FRB, reducing  $F_\nu$  (more than it would increase  $\Delta t$ ),  $T_{scatt}$  and  $S/N$ . Zhang, Wang & Kontar (2021) estimate scattering widths  $\Delta t \sim 0.5$  s at 150 MHz, that would reduce  $S/N$  by an additional factor  $\sim 20$  in comparison to an unbroadened  $\Delta t \sim 1$  ms.

It is evident that a Galactic FRB would have to have flux  $\gtrsim$  GJy for its Solar reflection to be detectable above the coronal thermal emission. Although such an event would be unprecedented, a 1 Jy FRB at  $z \sim 1$  would have a flux  $\sim 100$  GJy at 10 kpc, indicating that such events may occur. Events producing 0.01–0.1 Jy at “cosmological” distances would be 1–10 GJy at Galactic distances, are more frequent than the most extreme events, and their Solar reflections are likely detectable.

#### 4 DISCUSSION

Figs. 2 and 3 show that for frequencies  $\nu \gtrsim 150$  MHz the reflectivity is substantial only for angles of incidence  $\theta \gtrsim 60^\circ$ . The fraction of the sky with angles of incidence  $\geq \theta$  is  $(1 + \cos 2\theta)/2$ , which is 0.25 for  $\theta = 60^\circ$  but only 0.12 for  $\theta = 70^\circ$ . Unlike the Moon, the Sun is a far-from-isotropic reflector at those frequencies and effectively reflects only a fraction of isotropically distributed sources, such as FRB. At lower frequencies  $\nu \lesssim 100$  MHz, the Sun is a good reflector, better than the Moon (Katz 2020), at all angles of incidence.

The results of this study were disappointing because of the intense background of Solar coronal thermal emission. This is in contrast to the results of our earlier study of Lunar scattering; the Lunar surface is only a weak source of thermal emission at radio frequencies.

#### ACKNOWLEDGEMENT

We thank an anonymous reviewer for several rounds of constructive criticism and for pointers to the Solar physics literature with which we were unfamiliar. In particular, we appreciate his calling to our attention the intense thermal coronal background that determines the observability of Solar reflections.

#### DATA AVAILABILITY

This theoretical study did not generate any new data.

#### REFERENCES

- Ananthakrishnan, S. 1995 *J. Astrophys. Astr.* 16, 427.  
 Bochenek, C., McKenna, D. L., Belov, K. V. *et al* 2020a *PASP* 132, 4202.  
 Bochenek, C., Ravi, V., Belov, K. V. *et al.* 2020b *Nature* 587, 59.  
 Brau, C. A. *Modern Problems in Classical Electrodynamics* 2004 Oxford U. Press, New York.  
 CHIME/FRB Collaboration, Andersen, B. C., Bandura, K. *et al.* 2019b *ApJ* 885, L24.  
 CHIME/FRB Collaboration, Andersen, B. C., Bandura, K. *et al.* 2020a *Nature* 587, 54.  
 CHIME/FRB Collaboration 2021a <http://chime-experiment.ca/en> accessed Oct. 27, 2021.  
 CHIME/FRB Collaboration, Amiri, M. *et al.* 2021b [arXiv:2106.04352](https://arxiv.org/abs/2106.04352).  
 Cordes, J. M. & Chatterjee, S. 2019 *ARA&A* 57, 417.  
 Fonseca, E., Andersen, B. C., Bhardwaj, M. *et al.* 2020 *ApJ* 891, L6.  
 Geryaev, F., Slamzin, V., Vainshtein, L. & Williams, D. R. 2014 *ApJ* 781, 200.  
 Katz, J. I. 2014 *Phys. Rev. D* 89, 103009.  
 Katz, J. I. 2020 *MNRAS* 494, 3464 [arXiv:2002.03506](https://arxiv.org/abs/2002.03506).  
 Kraus, J. D. 1966 *Radio Astronomy* McGraw-Hill, New York.  
 de Lera Acedo, E., Pienaar, H., Ghods, N. R. *et al.* 2020 [arXiv:2003.12744v2](https://arxiv.org/abs/2003.12744v2).  
 McCauley, P. I., Cairns, I. H. & Morgan, J. 2018 *Solar Phys.* 293, 132.  
 Mercier, C. & Chambe, G. 2015 *A&A* 583, A101.  
 Mondal, S., Oberoi, D. & Mohan, A. 2020 *ApJ* 895, L39.  
 Newkirk, G. Jr. 1961 *ApJ* 133, 983.  
 Newkirk, G. Jr. 1967 *ARA&A* 5, 213.  
 Ng, C., Vanderlinde, K., Paradise, A. *et al.* 2017 [arXiv:1702.04728](https://arxiv.org/abs/1702.04728).  
 Pastor-Marazuela, I., Connor, L., van Leeuwen, J. *et al.* 2020 [arXiv:2010.14334](https://arxiv.org/abs/2010.14334).  
 Petroff, E., Barr, E. D., Jameson, A. *et al.* 2016 <http://www.frbcat.org>; see also Transient Name Server.  
 Petroff, E., Hessels, J. W. T. & Lorimer, D. R. 2022 *Astron. & Ap. Rev.* in press [arXiv:2107.10113](https://arxiv.org/abs/2107.10113).  
 Pleunis, Z., Michilli, D., Bassa, C. G. *et al.* 2021 *ApJ* 911, L3.  
 Saito, K., Poland, A. I. & Munro, R. H. 1977 *Solar Phys.* 55, 121.  
 Spitzer, L. *Physics of Fully Ionized Gases* 1962 (Interscience, New York).  
 Tingay, S. J., Goeke, R., Bowman, J. D. *et al.* 2013 *Pub. Astr. Soc. Australia* 30, e007.  
 Transient Name Server 2021 <https://wis-tns.weizmann.ac.il> accessed October 27, 2021.  
 van Haarlem, M. P., Wise, M. W., Gunst, A. W. *et al.* 2013 *A&A* 556, A2.  
 van Hoof, P. A. M., Williams, R. J. R., Volk, K. *et al.* 2014 *MNRAS* 444, 420.  
 Wayth, R. B., Tingay, S. J., Trott, C. M. *et al.* 2018 *Pub. Astro. Soc. Australia* 35, e033.  
 Xhang, P., Wang, C. B. & Kontar, E. P. 2021 *ApJ* 909, 195.